AJNR

A Physiological Barrier Distal to the Anatomic Blood-Brain Barrier in a Model of Transvascular Delivery

Leslie L. Muldoon, Michael A. Pagel, Robert A. Kroll, Simon Roman-Goldstein, Russell S. Jones and Edward A. Neuwelt

AJNR Am J Neuroradiol 1999, 20 (2) 217-222
http://www.ajnr.org/content/20/2/217

AJNR Am J Neuroradiol 20:217–222, February 1999

A Physiological Barrier Distal to the Anatomic Blood-Brain Barrier in a Model of Transvascular Delivery

Leslie L. Muldoon, Michael A. Pagel, Robert A. Kroll, Simon Roman-Goldstein, Russell S. Jones, and Edward A. Neuwelt

BACKGROUND AND PURPOSE: **Osmotic disruption of the blood-brain barrier (BBB) provides a method for transvascular delivery of therapeutic agents to the brain. The apparent global delivery of viral-sized iron oxide particles to the rat brain after BBB opening as seen on MR images was compared with the cellular and subcellular location and distribution of the particles.**

METHODS: **Two dextran-coated superparamagnetic monocrystalline iron oxide nanoparticle contrast agents, MION and Feridex, were administered intraarterially in rats at 10 mg Fe/kg immediately after osmotic opening of the BBB with hyperosmolar mannitol. After 2 to 24 hours, iron distribution in the brain was evaluated first with MR imaging then by histochemical analysis and electron microscopy to assess perivascular and intracellular distribution.**

RESULTS: **After BBB opening, MR images showed enhancement throughout the disrupted hemisphere for both Feridex and MION. Feridex histochemical staining was found in capillaries of the disrupted hemisphere. Electron microscopy showed that the Feridex particles passed the capillary endothelial cells but did not cross beyond the basement membrane. In contrast, after MION delivery, iron histochemistry was detected within cell bodies in the disrupted hemisphere, and the electron-dense MION core was detected intracellularly and extracellularly in the neuropil.**

CONCLUSION: **MR images showing homogeneous delivery to the brain at the macroscopic level did not indicate delivery at the microscopic level. These data support the presence of a physiological barrier at the basal lamina, analogous to the podocyte in the kidney, distal to the anatomic (tight junction) BBB, which may limit the distribution of some proteins and viral particles after transvascular delivery to the brain.**

The blood-brain barrier (BBB) consists of a continuous layer of cerebral vascular endothelial cells bound together with tight junctions that prevent access of most blood-borne agents to the brain (1, 2). Intracarotid infusion of hypertonic mannitol results in transient shrinkage of cerebrovascular endothelial cells with subsequent increased permeability of the tight junctions (3, 4). Osmotic BBB disruption is used clinically as a means of increasing delivery of chemotherapeutic agents for the treatment of brain tumors (1, 5).

The BBB disruption technique may be useful for global delivery of new therapeutic agents to the brain, such as viral vectors for gene therapy. In previous studies, no delivery of either herpesvirus or adenovirus to the rat brain could be detected in control animals without osmotic BBB opening; after BBB disruption, transvascular delivery of both vectors to the brain has been demonstrated with radiolabeled virions and by immunostaining for transgenic protein expression (6–9). However, viral particles may be limited in their delivery because they are very large (10–150 nm diameter) in relation to chemotherapeutic drugs and imaging agents that have been delivered across the BBB (6–9). Additionally, binding to proteins, membranes, or specific receptors may limit delivery of gene therapy vectors across the BBB and distribution through brain parenchyma after BBB disruption.

To explore the delivery of viral-sized particles across the BBB in a rodent model of BBB disruption,

Received July 1, 1998; accepted after revision October 27.

Supported by a Veterans Administration merit review grant, and by grants CA31770 from the National Cancer Institute and NS34608 and NS33618 from the National Institutes of Neurological Disorders and Stroke.

From the Departments of Cell and Developmental Biology (L.L.M.), Neurology (L.L.M., R.A.K., E.A.N.), Radiology (S.R-G.), and Pathology (R.S.J.), and the Division of Neurosurgery (E.A.N.), Oregon Health Sciences University, Portland; and The Veterans Administration Medical Center, Portland, (M.A.P., E.A.N.).

Address reprint requests to Edward A. Neuwelt, MD, Blood-Brain Barrier Program L603, Oregon Health Sciences University, 3181 SW Sam Jackson Park Rd, Portland, OR

we used superparamagnetic dextran-coated monocrystalline iron oxide particles with sizes of the same order of magnitude as viral particles (10–13). The distribution of these particles can be monitored by MR imaging and then by histochemical staining for iron and electron microscopy of the electron-dense core (14). The MION particles (Combidex, Advanced Magnetics, Cambridge, MA) developed by Weissleder et al are homogeneous in size (20 ± 4 nm hydrodynamic diameter) and consist of monocrystalline iron oxide completely surrounded by a dextran coat derived from 10,000 molecular weight dextran subunits (10, 11). The MION complexes are not readily phagocytized, protein bound, or membrane bound, and have a half-life of 24 hours in humans (10, 11). Delivery of MION across the BBB has been exhibited only after osmotic opening (7, 12). Feridex (Feridex I.V., Advanced Magnetics), in comparison, has a wider size range, and the dextran coat on the Feridex iron oxide crystal is incomplete and variable in extent (13, 14). Feridex is rapidly opsonized, and thus represents a class of agents (proteins, viral vectors, etc) that are recognized by the scavenger systems protecting the body from noxious compounds. Because of the similarity of sizes and because gene therapy vectors and iron oxide particles require breaching of the BBB to enter the brain, the iron particles provide a valuable tool to assess the possible distribution and location of viral vectors after osmotic BBB disruption.

Methods

All animal experimentation was performed in accordance with institutional guidelines.

Intracerebral Inoculation into Rat Brain

Inoculation of the iron oxide compounds into rat brain was performed to assess the distribution and cellular uptake of the agents when delivered in a manner similar to that in viral vector studies, bypassing the BBB (7, 8). Rats (n = 4) were anesthetized with intraperitoneal ketamine (60 mg/kg) and diazepam (7.5 mg/kg). A 2-mm-diameter hole was drilled in the skull and a 27-gauge needle was slowly lowered into the right caudate putamen using coordinates as follows: bregma = 0; lateral = −0.31, vertical = −0.65). Infusion of 24 μL of saline containing Feridex (10 μg Fe, n = 2) or MION (10 μg Fe, n = 2) was performed over a 20-minute period to avoid loss out of the needle track. The needle was withdrawn over a 5-minute period, the burr hole was sealed with bone wax, and the scalp was sutured. MR imaging was performed 24 hours after iron administration, and brain sections were assessed by histochemistry for iron, as described below.

BBB Disruption Studies

Osmotic BBB disruption was performed to assess transvascular delivery of iron oxide nanoparticles. Rats (n = 15) were anesthetized with 2% isoflurane (AErrane; Anaquest, Madison, WI), then switched to propofol (650 μg/kg/min, Zeneca Pharmaceuticals, Wilmington, DE). The carotid artery was catheterized, and 37°C 25% mannitol (for rats in the BBB disruption group) or normal saline (control group) was infused cephalad into the right internal carotid artery, as described previously (7–9). To provide a qualitative measure of the degree of barrier opening, Evans blue dye (2%, 2 mL/kg, Sigma Chem Co, St Louis, MO) was administered intravenously prior to infusion of mannitol or saline. All animals in the BBB disruption group displayed 2+ or 3+ staining, indicating good to excellent barrier opening. Immediately after infusion of mannitol or saline, the rats received either Feridex (10 mg Fe/kg, n = 6; 20 mg Fe/kg, n = 2) or MION (10 mg Fe/kg, n = 7) in 1.5-mL saline delivered via the carotid cannula over 1 minute. The experimental treatment for each animal in this study is shown in the Table.

Experimental protocols for rats with disruption of blood-brain barrier

Agent/Delivery	MR Imaging	Electron Microscopy	Histology
MION (n = 7) + mannitol	○ ⟶	○	
		○	
	○ ⟶		○
			○, ○, ○
			○ (2 hr)
Feridex (n = 4) saline control	○ ⟶	○	
	○ (20) →	○	
			○, ○
Feridex (n = 4) + mannitol	○, ○ →	○, ○	
	○ ⟶		○
	○ (20) ⟶		○

Note.—Circles indicate rats that were given either MION or Feridex administered intraarterially after saline or mannitol for BBB disruption. Animals received 10 mg/kg of iron, except for the two animals that received 20 mg/kg. Animals were imaged and analyzed 24 hours after iron administration, except for one animal that was assessed at 2 hours. Arrows indicate that the same rat was evaluated by MR imaging and by electron microscopy or histology.

MR Imaging

Twenty-four hours after receiving iron oxide particles by intracerebral inoculation or with BBB disruption, rats were anesthetized with ketamine (60 mg/kg) and valium (7.5 mg/kg) for MR imaging. Coronal MR images were obtained with a 9-mm field of view, a 256 × 192 matrix, and two excitations. T1-weighted images were obtained with a TR/TE of 500/13 and a 3-mm section thickness. Although not shown, fast spin-echo T2-weighted images were obtained with a TR/TE_{eff} of 3000/95 and a 3-mm section thickness.

Histochemical Staining

Immediately after MR imaging, or 2 hours or 24 hours after iron administration (see Table), rats were killed with a barbiturate overdose and their brains were immersion-fixed in neutral buffered formalin for histochemical analysis (n = 13). Serial coronal sections (100 μm) from throughout the brain were cut on a Vibratome. Iron histochemical staining was performed on 10 to 12 sections from each brain as described previously (7, 12). Iron staining was evaluated by four of the authors, who were not blinded to the experimental treatment.

Electron Microscopy

Immediately after MR imaging, or 24 hours after iron administration (see Table), rats were killed with a barbiturate overdose and their brains were immersion-fixed in glutaraldehyde for ultrastructural analysis (n = 6). Tissues were washed in 0.1 M sodium cacodylate for 25 minutes, postfixed in 2% osmium tetroxide, dehydrated in ascending concentrations of ethanol, and embedded in Epon 812. Unstained ultrathin sections were examined on a Philips EM 301 transmission electron microscope (Philips Elec-

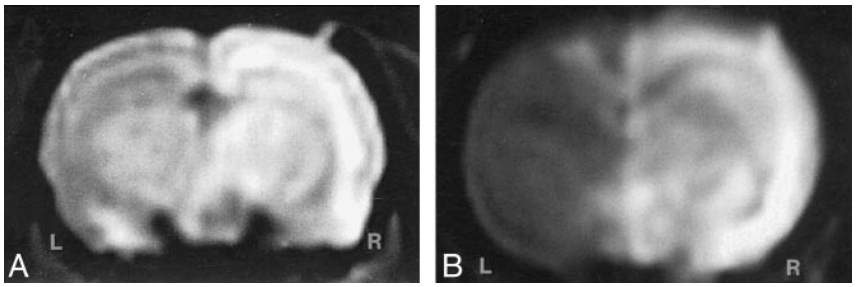

FIG 1. MR imaging of transvascular delivery of Feridex and MION in the rat brain.

A, T1-weighted image obtained 24 hours after osmotic BBB disruption and intracarotid administration of Feridex (10 mg Fe/kg) shows enhancement in the right cerebral hemisphere.

B, T1-weighted image 24 hours after administration of MION (10 mg Fe/kg) with BBB disruption. The disrupted right cerebral hemisphere (R) enhances (white) with iron, while the left hemisphere (L) shows the noncontrast-enhanced rat brain.

tronics, Einhoven, the Netherlands). Electron microscopy was performed by one of the authors, who was blinded to the experimental conditions, and results were interpreted by all the authors.

Results

In the initial experiment, we investigated whether Feridex and MION could be detected by MR imaging 24 hours after focal intracerebral inoculation into the rodent brain. T1-weighted MR images showed intense signal dropout over a large volume surrounding the injection site, which was similar to the images previously reported for MION 2 hours after inoculation (12). Histochemical staining for iron was detected in both gray and white matter extending approximately 2 mm from the injection site. We have previously found that MION is rapidly taken up by cells after direct inoculation, resulting in intense staining of neurons (12). After Feridex delivery, iron staining was detected in scattered cell bodies that, morphologically, appeared to be neurons, although this was less intense and widespread than in previous MION results. Thus, it appeared that Feridex and MION behaved similarly after intracerebral inoculation.

To assess transvascular delivery of particles, we administered intracarotid mannitol to open the BBB in the experimental animals or saline in the control group, immediately followed by intracarotid infusion of iron oxide nanoparticles. The saline control animals were imaged 24 hours after Feridex infusion, and no enhancement was seen on MR images and no difference was found between the infused right hemisphere and the contralateral left hemisphere. Four animals given Feridex and two animals given MION with osmotic opening were imaged 24 hours after BBB disruption. On T1-weighted MR images (Fig 1), the presence of the superparamagnetic iron oxide was indicated by signal enhancement (white). For both the Feridex (Fig 1A) and MION (Fig 1B) groups, delivery with osmotic BBB disruption resulted in increased signal throughout most of the disrupted hemisphere. On T2-weighted fast spin-echo sequences (not shown), in which iron was detected as reduced signal (black), the most notable changes occurred in the more highly vascularized basal ganglia. The distribution of Feridex in the rat brain after BBB disruption, as determined by studying the MR images, was qualitatively identical to the distribution of MION when delivered with BBB disruption.

The brain sections obtained 24 hours after intraarterial infusion of Feridex or MION were stained for the presence of iron. In the control animals, no difference in iron staining was detected between the right and left hemispheres when Feridex was infused after saline, demonstrating that Feridex did not enter the brain in animals with a normal BBB. This result is in agreement with previously published studies showing that MION at 100 mg/kg does not cross the normal BBB. In animals receiving Feridex after infusion of hyperosmotic mannitol to disrupt the BBB, no staining was detected within cells that could be morphologically identified as neurons or glial cells. However, capillary staining was detected throughout the disrupted hemisphere, with some degree of crossover along the midline (Fig 2A). This staining was limited to the capillary walls, appeared to be diffuse throughout the endothelial cells, and was clearly distinct from red blood cell staining (Fig 2B). The lack of capillary staining in control animals and in the contralateral nondisrupted hemisphere in BBB disruption animals suggests that this staining does not represent extracellular binding of iron to the capillary lumen.

The histochemical findings in the animals receiving Feridex differed from the staining seen in animals that were given MION with BBB disruption. At 2 hours after BBB disruption, capillary, interstitial, and cellular staining for iron was detected in the disrupted hemisphere (Fig 2C). By 24 hours after MION delivery, staining for iron was found within cell bodies throughout the disrupted hemisphere, and some capillary staining was detected in the disrupted hemisphere (Fig 2D), similar to the staining in the Feridex brains, but the majority of capillaries did not stain. The results with 10 mg/kg MION are qualitatively similar, although less intense than the previously published histologic findings after administration of 100 mg/kg MION, in which cell bodies, processes, and fiber tracks all clearly stained for iron (12).

Electron microscopy was performed to document the distribution of iron oxide particles in the brain. No iron oxide particles were detected in the brain of control animals that received Feridex after saline

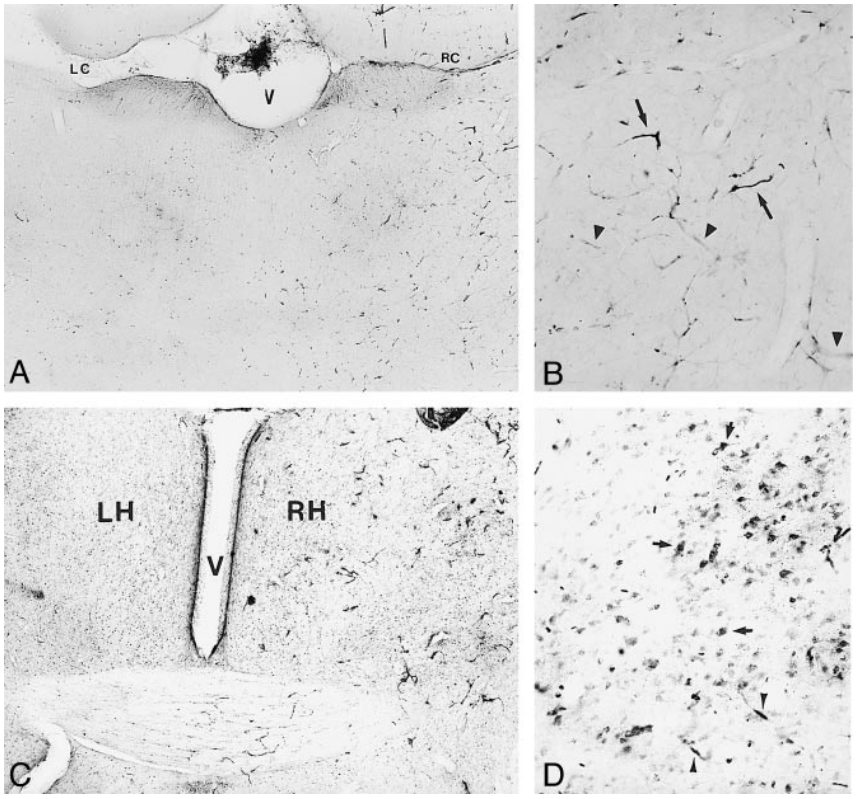

FIG 2. Light microscopy of transvascular delivery of iron oxide particles in the rat brain.

A, Histochemical staining for iron after delivery of Feridex (10 mg Fe/kg) with BBB disruption. Iron staining is increased in the disrupted right cerebral hemisphere compared with the contralateral nondisrupted left hemisphere, or saline controls. V = ventricle, LC = left corpus callosum and ventricle, RC = right corpus callosum (original magnification ×20).

B, Capillary staining for iron in right cerebral hemisphere after Feridex delivery with BBB disruption is indicated by *arrowheads. Arrows* indicate staining of red blood cells (original magnification ×50).

C, Histochemical staining for iron in rat brain 2 hours after delivery of MION (10 mg Fe/kg) with BBB disruption shows an increase in iron staining in the disrupted right cerebral hemisphere (RH) compared with the nondisrupted left hemisphere (LH). V indicates the ventricle (original magnification ×20).

D, Cellular staining for iron (*arrows*) is widespread in the right cerebral hemisphere 24 hours after delivery of 10 mg/kg MION with BBB disruption. *Arrowheads* indicate capillary staining (original magnification ×100).

infusion. Electron microscopy demonstrated delivery of Feridex across the anatomic BBB only after osmotic BBB disruption (Fig 3A). In animals with BBB disruption who were given Feridex, iron oxide particles were clearly present between the capillary endothelial cells and the basement membrane (Fig 3B). In rare instances, electron-dense particles were detected intracellularly in either the endothelial cells or in pericytes located next to the basement membrane (Fig 3C). No Feridex particles were detected in the extracellular space or within cells in the brain parenchyma after BBB disruption.

In contrast to Feridex, MION particles were found predominantly intracellularly in the disrupted hemisphere (Fig 3D and E). Although not clearly intracellular in Figure 3D, MION was found near mitochondria and synapses rather than adjacent to a capillary. MION was found in pericytes around capillaries (Fig 3E), but no MION was found bound to or blocked by the basement membrane.

Discussion

Feridex delivery to brains with BBB disruption appeared homogeneous when assessed by MR imaging, and was visually similar to the distribution of MION. Thus, when assessed at the level of the whole brain, it appeared that both agents crossed the osmotically open BBB into the brain parenchyma. Yet, on a microscopic level, although Feridex particles crossed the anatomic BBB, they stopped at the basement membrane and did not in fact enter the brain. The MION particles were not stopped at the basal lamina and had much freer access to the brain parenchyma. We propose the terms *stealth* and *nonstealth* to indicate agents that do or do not cross the basement membrane, respectively.

The difference between macroscopic and microscopic findings points out the problem of extrapolating whole-brain data to the cellular level. These results bring into question the results of studies designed to assess delivery of agents across the BBB. For example, whole-brain homogenates might incorrectly be interpreted to indicate penetration into brain. Even when care is taken to exclude the capillaries from the brain homogenate, as in the capillary depletion procedure (15), it is unclear whether proteins bound to or trapped by the basal lamina are considered to be in the capillary fraction or the brain fraction. It is possible that capillary depletion, used to assess receptor-mediated transport of therapeutic proteins across the BBB (1, 16), may incorrectly show nonstealth agents to be within the brain. As another example, passage of radiolabeled agents across the BBB has been assessed by quantitative autoradiography of whole-brain sections, with approximately the same level of resolution as MR images (17). It is possible that whole-brain autoradiography, like MR imaging, may also be incorrectly interpreted to indicate distribution of agents, such as Feridex, throughout the parenchyma.

The current findings with the nonstealth Feridex particles are supported by other studies showing that some agents may be bound to the basal lamina rather than pass through the BBB into the brain. In one study of osmotic disruption in the rat, serum

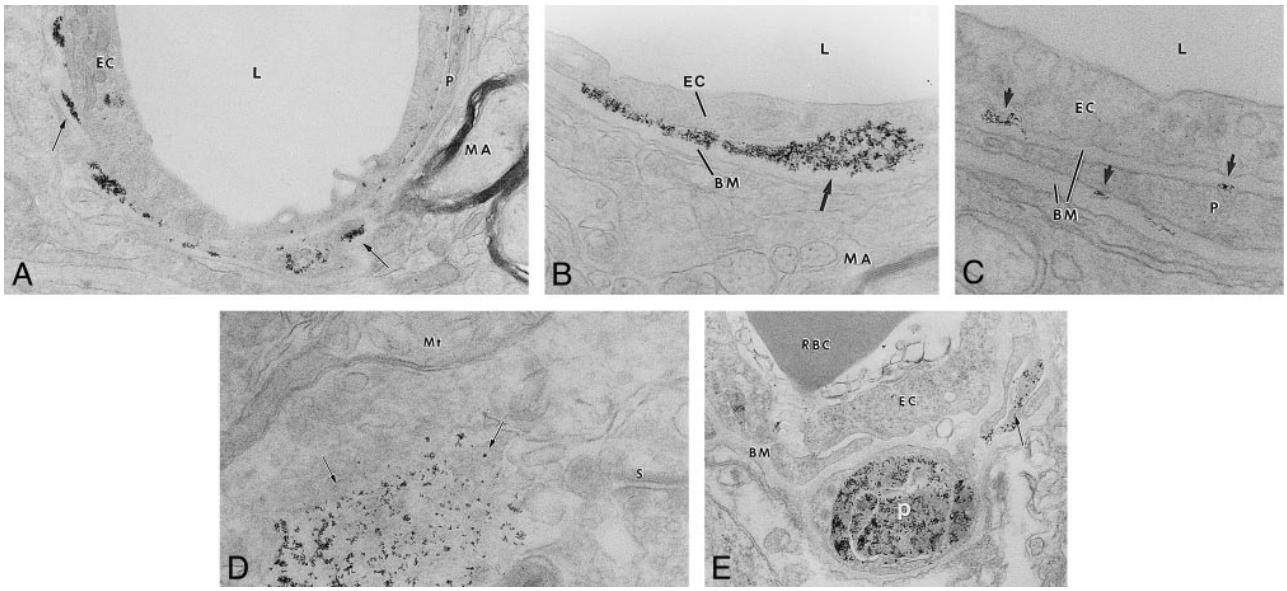

FIG 3. *A–E,* Electron microscopy of transvascular delivery of iron particles. Rat brain micrographs after BBB disruption-enhanced delivery of Feridex are shown in *A* (original magnification ×19,000), *B* (original magnification ×48,000), and *C* (original magnification ×87,000). Electron-dense particles (*arrows*) are located around capillaries, adjacent to the basement membrane (BM) and pericapillary pericyte (P). L = capillary lumen, MA = myelinated axon, EC = capillary endothelial cell. Location of MION after BBB disruption is shown in *D* (original magnification ×65,000) and *E* (original magnification ×36,700). Electron-dense MION particles (*D, arrows*) were found near synapses (S) and mitochondria (Mt). MION particles were detected in pericapillary pericytes (P) and in what appear to be pericyte processes (*E, arrow*). EC = capillary endothelial cell, RBC = red blood cell, BM = basement membrane.

albumin only very slowly entered the neuropil, although high concentrations were detected at the basement membrane (18). In a study of immunoglobulin localization at the BBB, immunohistochemistry and electron microscopy were used to demonstrate that immunoglobulin molecules were concentrated along the basal lamina of the brain microvasculature (19). Even when such proteins as CD4 are shuttled directly across the BBB using the transferrin receptor, they appear to be heavily localized to the capillaries (16). We have previously documented delivery of recombinant virus across the BBB, but, interestingly, marker staining appeared to be primarily in glial cells with pericapillary foot processes, suggesting that gene therapy vectors may also be blocked or slowed by the basement membrane (6). These results challenge the view that once agents have crossed the BBB they have access to the entire brain.

If blockage of agents at the level of the basal lamina is more prevalent than previously thought, the issue now is the mechanism of this blockage and the properties of agents that promote their binding to the basal lamina. Size alone does not explain the difference in delivery of stealth and nonstealth agents, as Feridex particles include the same size particles as MION, in addition to particles up to 150 nm in diameter (13, 14). Herpesvirus vectors with sizes up to 150 nm diameter can be delivered transvascularly (7, 8). Our hypothesis is that agents that are rapidly protein bound or membrane bound are more likely to be trapped by the basement membrane. Feridex is known to opsonize rapidly, in contrast to MION (11, 13, 14). Alternatively, the mechanism may have to do with the slightly negative electrostatic charge of the particles due to the carboxylic groups of dextran (12). Binding of negatively charged agents by carbohydrate groups has been demonstrated on renal glomerular podocytes (20). In the brain, such trapping may be an important protective mechanism, as the only CNS macrophage, the microglial cell, also localizes in the perivascular region (21).

Until the demonstration in the 1960s by Brightman of the anatomic BBB at the tight junction between capillary endothelial cells, the structural basis of the BBB was thought to be at the level of the astrocyte foot processes and basal lamina surrounding brain capillaries (1, 3). This older view should be reassessed, at least for some agents. Aspects of the BBB beyond the endothelial tight junctions may play a role in restricting access of agents to the brain.

Conclusion

Our results establish the existence of a second physiological barrier to the passage of agents from the blood to the brain, at the level of the basal lamina. This barrier may trap opsonized proteins and viral vectors after transvascular delivery and eliminate them via perivascular microglial cells (macrophages [21]). These results may impact the use of osmotic BBB disruption and other methods for circumventing the BBB for the delivery of therapeutic proteins and viral vectors to the brain.

Acknowledgments

We thank Ralph Weissleder for providing the MION used in this study, Lisa Bennett for histologic expertise, and Patrice

Manley and Kathy Griffith for technical assistance with MR imaging. We also thank Randal Nixon and Lee Josephson for assistance in interpreting the electron micrographs.

References

1. Kroll RA, Neuwelt EA. **Outwitting the blood-brain barrier for therapeutic purposes: osmotic opening and other means.** *Neurosurgery* 1998;42:1083–1100
2. Pardridge WM. **Drug delivery to the brain.** *J Cereb Blood Flow Metab* 1997;17:713–731
3. Brightman MW, Hori M, Rapoport SI, Reese TS, Westergaard E. **Osmotic opening of tight junctions in cerebral endothelium.** *J Comp Neurol* 1973;152:317–326
4. Rapoport SI, Robinson PJ. **Tight-junctional modification as the basis of osmotic opening of the blood-brain barrier.** *Ann N Y Acad Sci* 1986;481:250–267
5. Dahlborg SA, Henner WD, Crossen JR, et al. **Non-AIDS primary CNS lymphoma: the first example of durable response in a primary brain tumor using enhance chemotherapy delivery without cognitive loss and without radiotherapy.** *Cancer J Sci Am* 1996;2:166–174
6. Doran SE, Dan Ren X, Betz AL, et al. **Gene expression from recombinant viral vectors in the CNS following blood-brain barrier disruption.** *Neurosurgery* 1995;36:965–970
7. Muldoon LL, Nilaver G, Kroll RA, et al. **Comparison of intracerebral inoculation and osmotic blood-brain barrier disruption for delivery of adenovirus, herpesvirus and iron oxide particles to normal rat brain.** *Am J Pathol* 1995;147:1840–1851
8. Nilaver G, Muldoon LL, Kroll RA, et al. **Delivery of herpesvirus and adenovirus to nude rat intracerebral tumors following osmotic blood-brain barrier disruption.** *Proc Natl Acad Sci U S A* 1995;92:9829–9833
9. Neuwelt EA, Pagel MA, Dix RD. **Delivery of UV-inactivated [35S]-herpesvirus across the BBB after osmotic modification.** *J Neurosurg* 1991;74:475–479
10. Weissleder R, Elizondo G, Wittenberg J, Rabito CA, Bengele HH, Josephson L. **Ultrasmall superparamagnetic iron oxide: characterization of a new class of contrast agents for MR imaging.** *Radiology* 1990;175:489–493
11. Shen T, Weissleder R, Papisov M, Bogdanov A Jr, Brady TJ. **Monocrystalline iron oxide nanocompounds (MION): physicochemical properties.** *Magn Reson Med* 1993;29:599–604
12. Neuwelt EA, Weissleder R, Nilaver G, et al. **Delivery of virus-sized iron oxide particles to rodent CNS neurons.** *Neurosurgery* 1994;34:777–784
13. Jung CW. **Surface properties of superparamagnetic iron oxide MR contrast agents: ferumoxides, ferumoxtran, ferumoxsil.** *Magn Reson Imaging* 1995;13:675–691
14. Jung CW, Jacobs P. **Physical and chemical properties of superparamagnetic iron oxide MR contrast agents: ferumoxides, ferumoxtran, ferumoxsil.** *Magn Reson Imaging* 1995;13:661–674
15. Triguero D, Buciak J, Pardridge WM. **Capillary depletion method for quantification of blood-brain barrier transport of circulating peptides and plasma proteins.** *J Neurochemistry* 1990; 54:1882–1888
16. Walrus LR, Pardridge WM, Starzyk RM, Friden PM. **Enhanced uptake of rsCD4 across the rodent and primate blood-brain barrier after conjugation to anti-transferrin receptor antibodies.** *J Pharmacol Exp Ther* 1996;277:1067–1075
17. Matsukado K, Inamura T, Nakano S, Fukui M, Bartus RT, Black KL. **Enhanced tumor uptake of carboplatin and survival in glioma-bearing rats by intracarotid infusion of bradykinin analog, RMP-7.** *Neurosurgery* 1996;39:125–133
18. Vorbrodt AW, Dobrogowska DH, Tarnawski M, Lossinsky AS. **A quantitative immunocytochemical study of the osmotic opening of the blood-brain barrier to endogenous albumin.** *J Neurocytol* 1994;23:792–800
19. Aihara N, Tanno H, Hall JJ, Pitts LH, Noble LJ. **Immunocytochemical localization of immunoglobulins in the rat brain: relationship to the blood-brain barrier.** *J Comp Neurol* 1994;342: 481–496
20. Mundel P, Kriz W. **Structure and function of podocytes: an update.** *Anat Embryol* 1995;192:385–397
21. Gehrmann J, Matsumoto Y, Kreutzberg GW. **Microglia: intrinsic immuneffector cell of the brain.** *Brain Res Rev* 1995;20:269–287

Please see the editorial on page 186 of this issue.